Efficient in vivo gene editing using ribonucleoproteins in skin stem cells of recessive dystrophic epidermolysis bullosa mouse model

Wenbo Wu[a,b], Zhiwei Lu[b], Fei Li[b], Wenjie Wang[b], Nannan Qian[b], Jinzhi Duan[b], Yu Zhang[b], Fengchao Wang[b], and Ting Chen[b,1]

[a]Peking University–Tsinghua University–National Institute of Biological Sciences Joint Graduate Program, School of Life Sciences, Peking University, Beijing 100871, China; and [b]National Institute of Biological Sciences, Beijing 102206, China

Edited by Brigid L. M. Hogan, Duke University Medical Center, Durham, NC, and approved December 23, 2016 (received for review September 2, 2016)

The prokaryotic CRISPR/Cas9 system has recently emerged as a powerful tool for genome editing in mammalian cells with the potential to bring curative therapies to patients with genetic diseases. However, efficient in vivo delivery of this genome editing machinery and indeed the very feasibility of using these techniques in vivo remain challenging for most tissue types. Here, we show that nonreplicable Cas9/sgRNA ribonucleoproteins can be used to correct genetic defects in skin stem cells of postnatal recessive dystrophic epidermolysis bullosa (RDEB) mice. We developed a method to locally deliver Cas9/sgRNA ribonucleoproteins into the skin of postnatal mice. This method results in rapid gene editing in epidermal stem cells. Using this method, we show that Cas9/sgRNA ribonucleoproteins efficiently excise exon80, which covers the point mutation in our RDEB mouse model, and thus restores the correct localization of the collagen VII protein in vivo. The skin blistering phenotype is also significantly ameliorated after treatment. This study provides an in vivo gene correction strategy using ribonucleoproteins as curative treatment for genetic diseases in skin and potentially in other somatic tissues.

in vivo gene editing | Cas9/sgRNA ribonucleoproteins | skin stem cell | electroporation | RDEB

CRISPR/Cas9-mediated genome editing has recently emerged as a powerful tool for genome engineering and for use as a potential therapeutic method to treat patients with genetic diseases (1–3). CRISPR/Cas9-mediated somatic genome editing of multiple mice organs, including lung, liver, brain, pancreas, and muscle, have been reported (4–10). To date, most approaches have relied on virus-based delivery systems, which have drawbacks such as potential integration of viral DNA into a host genome, off-target effects due to prolonged expression of genome editing machinery, and possible activation of virus-triggered host immune responses. Additionally, most therapeutic applications will require the tissue-specific delivery of the genome editing machinery in vivo. So far, this has remained challenging for most tissues, such as skin.

In healthy skin, epidermal keratinocytes and dermal fibroblasts secrete collagen VII protein and it in turn forms stable homotrimers to assemble into networks of anchoring fibrils (11, 12). The anchoring fibrils are located within the basement membrane zone (BMZ) between the epidermis and dermis, where they participate in stabilizing the association of the epidermis to the underlying dermis (13). In patients with recessive dystrophic epidermolysis bullosa (RDEB), mutations in the *Col7a1* gene cause absent or dysfunctional collagen VII protein production, which leads to defective epidermal–dermal adhesion (14). The main clinical manifestations of RDEB include: chronic and severe cutaneous blistering, especially on hands and feet; damage to internal epithelia, such as oral, esophageal, and anal structures; an increased risk for developing aggressive forms of squamous cell carcinoma; and overall reduced life expectancy (15).

Treatments currently under development for patients with RDEB mainly include protein therapy (16, 17) or combined gene and cell therapy. In particular, the cellular therapies of RDEB rely on introducing donor cells that are capable of producing normal collagen VII protein, such as allogeneic dermal fibroblasts, gene-corrected RDEB fibroblasts (18–20), gene-corrected keratinocytes in autografts (21–23), and gene-corrected keratinocytes derived from reverted-induced pluripotent stem cells (24–27). Based on what is known from these studies, clinical trials for RDEB that combine gene and cell therapies have been initiated. Examples include the intradermal injection of allogeneic fibroblasts (20) and the grafting of epidermal tissues generated ex vivo that express virally introduced normal collagen VII (28). Bone marrow transplantation has also been reported to ameliorate the skin blistering phenotype (29, 30). Despite all of these advances, there are still no curative treatments for RDEB.

Here, we demonstrate the in vivo use of Cas9/sgRNA ribonucleoproteins to mediate gene correction in skin stem cells of postnatal RDEB mice. First we generate a RDEB mouse model based on a patient-specific point mutation. Then we establish a mouse model missing the exon containing the point mutation in *Col7a1* gene to prove the efficiency and safety of exon skipping as a gene correction method. To apply the gene correction system in intact postnatal skin, we developed a method to deliver nonreplicable protein/RNA complexes in vivo; it induces one-time, permanent modification of genomic DNA in skin stem cells. Finally, we demonstrate the feasibility and efficiency of our

Significance

The prokaryotic CRISPR/Cas9 system has recently been applied in genome editing in mammalian cells with the potential to bring curative therapies to patients with genetic diseases. However, efficient in vivo delivery of this machinery remains challenging for most tissue types. We now developed a method to locally deliver Cas9/sgRNA ribonucleoproteins into the skin of postnatal mice, which was used to correct genetic defects in skin stem cells of postnatal recessive dystrophic epidermolysis bullosa (RDEB) mice. Our study provides proof-of-principle evidence that Cas9/sgRNA ribonucleoprotein-based gene therapies can be applied to restore collagen VII protein function in postnatal RDEB mice, suggesting that the Cas9/sgRNA ribonucleoprotein-based gene therapy may offer curative treatment for RDEB and other genetic disorders.

Author contributions: W. Wu and T.C. designed research; W. Wu, Z.L., F.L., W. Wang, and N.Q. performed research; J.D., Y.Z., and F.W. contributed new reagents/analytic tools; W. Wu and T.C. analyzed data; and W. Wu and T.C. wrote the paper.

The authors declare no conflict of interest.

This article is a PNAS Direct Submission.

Freely available online through the PNAS open access option.

[1]To whom correspondence should be addressed. Email: chenting@nibs.ac.cn.

This article contains supporting information online at www.pnas.org/lookup/suppl/doi:10.1073/pnas.1614775114/-/DCSupplemental.

curative gene editing system to permanently restore the function of the collagen VII protein in vivo.

Results

***Col7a1 c.6485G > A mut/mut* Mice Show RDEB Hallmarks.** First, we established a RDEB mouse model based on the genome sequencing data of a patient with RDEB in Beijing. CRISPR/Cas9 system-facilitated homologous recombination was used to generate the *c.6485G > A* point mutation within exon80 of the mouse *Col7a1* gene (Fig. 1*A*). Using specific primer pairs targeting wild-type (WT) and mutant alleles in PCR-based genotyping assays, we can distinguish among WT, heterozygous, and homozygous mutant mice (Fig. 1*B*). Sequencing of genomic DNA confirmed the existence of the expected specific *c.6485G > A* mutation within the *Col7a1* locus (Fig. 1*C*). After birth, *Col7a1 c.6485G > A mut/mut* mice exhibited striking skin blistering phenotypes similar to the patient with RDEB whose point mutation was used to create this mouse model (Fig. 1*D*). The *Col7a1 c.6485G > A wt/mut* mice appeared normal, consistent with the patient's carrier parent. Histological examinations demonstrated separation of the epidermis from the dermis at all of the locations examined, including the mouse tail, paw, and back skin (Fig. 1*E*). Collagen VII immunofluorescence staining revealed striking changes in protein-localization patterns: in WT skin, collagen VII proteins were localized at the BMZ in a linear pattern; in the *Col7a1 c.6485G > A mut/mut* skin, collagen VII proteins were scattered in a dotted pattern in the basal epidermis layer and the dermis near the BMZ zone (Fig. 1*F* and Fig. S1*A*). Most of the *Col7a1 c.6485G > A mut/mut* mice died within a week after birth, due to complications from the disease (Fig. S1*B*). Overall, our newly generated *Col7a1 c.6485G > A mut/mut* mouse line, based on a patient-specific point mutation, exhibits typical pathologic features encountered in patients with RDEB. And it is a disease-relevant animal model that can enable us to develop effective gene correction therapy.

Evidence from both an in Vivo Animal Model and an in Vitro Cell Line Demonstrates the Feasibility and Safety of Exon Skipping as a Gene Correction Method. *Col7a1* exon80 encodes part of the collagenous domain that contains stretches of bases coding for G-X-Y (G: glycine, X and Y: two other random amino acids) repeat sequences; it is in-frame with neighboring exons. In theory, deleting the point mutation containing exon80 should result in a collagen VII protein with a slightly shortened collagenous domain that would ostensibly retain its normal function (Fig. S2*A*). However, the feasibility and safety of this gene correction strategy must of course be tested rigorously in vivo, with particular attention paid to whether or not the shortened form of the collagen VII protein may act in a dominant negative manner to disrupt homotrimer formation. To this end, we generated *Col7a1* exon80-skipped mice (*Col7a1 Δexon80*) using the CRISPR/Cas9 system (Fig. 2*A*). In this mutant strain, there is an 8-bp deletion that spans the junction between intron79 and exon80 (3 bp in intron79 and 5 bp in exon80). This deletion abrogates the acceptor site for intron splicing and causes exon80 to be skipped during splicing. Genomic DNA and mRNA sequencing results confirmed, respectively, the occurrence of the 8-bp deletion at the *Col7a1* locus and the skipping of exon80 (Fig. 2 *B* and *C*). The *Col7a1 Δexon80 mut/mut* and importantly *wt/mut* mice are indistinguishable from their WT littermates; no skin blistering phenotypes were observed in newborns or in adults (Fig. 2*D*). The localization of the collagen VII protein was identical in *Col7a1 Δexon80 mut/mut* and *wt/mut*, and WT mice, exhibiting a linear pattern at the BMZ (Fig. 2*E*). Thorough histological examination revealed an intact epidermis and dermis adhesion at all of the locations examined, including the mouse

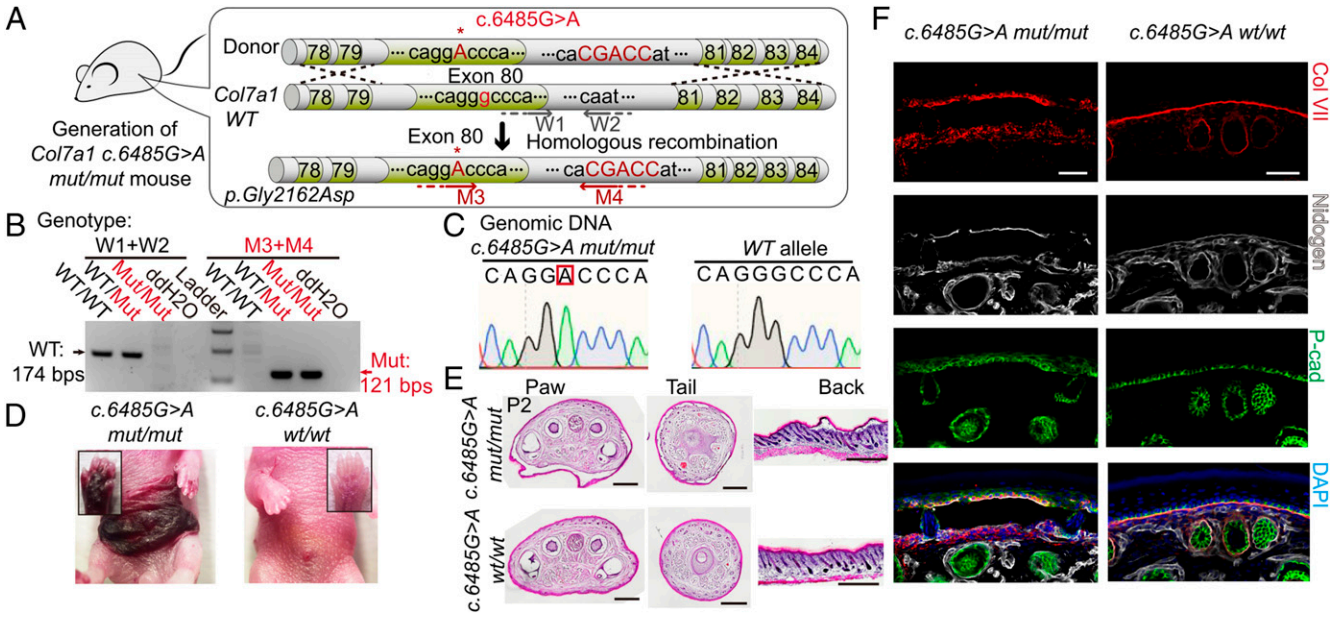

Fig. 1. Establishment of a RDEB mouse model based on patient-specific mutations. (*A*) A portion of the murine *Col7a1* gene from exon78 to exon 84 (about 1.5 kb) is used as the donor DNA to generate a knockin mouse line. *Col7a1 c.6485G > A* mutation in exon80 is highlighted with uppercase letters. A 5-bp (CGACC) insertion in intron80 was also introduced to facilitate genotyping identification of the mutant allele. The W1/W2 and M3/M4 primer pairs are used to identify the WT *Col7a1* locus and the recombined *Col7a1* locus, respectively. (*B*) Genotyping results of *Col7a1 c.6485G > A* WT (*wt/wt*), heterozygous (*wt/mut*), and homozygous (*mut/mut*) mice using the W1/W2 and M3/M4 primers. (*C*) Partial *Col7a1* locus genomic DNA sequencing results for WT and *Col7a1 c.6485G > A mut/mut* mice. (*D*) Spontaneous blisters form on the paws and ventral skin of *Col7a1 c.6485G > A mut/mut* mice. (*E*) H&E staining of postnatal day 2 (P2) *Col7a1 c.6485G > A mut/mut* and WT tissue sections from paw, tail, and back skin. Note the separation of epidermis from dermis in *Col7a1 c.6485G > A mut/mut* skins. (Scale bar, 500 μm.) (*F*) Immunofluorescence stainings of collagen VII (Col VII), P-cad, and Nidogen in *Col7a1 c.6485G > A mut/mut* and WT tail skins. (Scale bar, 50 μm.)

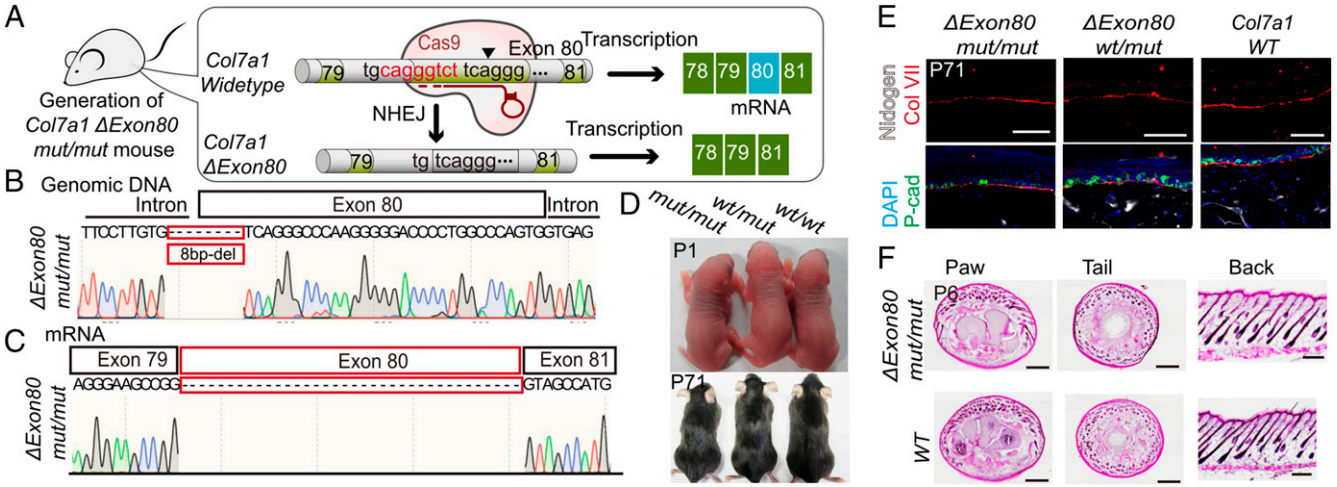

Fig. 2. *Col7a1-ΔExon80 mut/mut and wt/mut* mice have normal skin with correct collagen VII localization. (*A*) Schematic diagram of the generation of *Col7a1-ΔExon80 mut/mut* mice. (*B*) Partial *Col7a1* genomic DNA sequencing result shows the 8-bp deletion spanning the intron79 and exon80 junction in *Col7a1-ΔExon80 mut/mut* mice. (*C*) Partial *Col7a1* mRNA sequencing result shows skipping of exon80 in *Col7a1-ΔExon80 mut/mut* mice. (*D*) Images of *Col7a1-ΔExon80 mut/mut*, *wt/mut*, *and WT* mice at P1 and P71. (*E*) Immunofluorescence staining for Col VII, P-cad, and Nidogen in the paws of *Col7a1-ΔExon80 mut/mut*, *wt/mut*, and WT mice. (Scale bar, 50 μm.) (*F*) H&E staining of P6 *Col7a1-ΔExon80 mut/mut* and WT tissue sections in paw, tail, and back skin. (Scale bar, 500 μm.)

tail, paw, and back skin (Fig. 2*F*). These results demonstrate that exon80 deletion in vivo is an efficient and safe strategy to restore the function of the collagen VII protein.

To screen for sgRNA pairs that can efficiently and specifically mediate DNA excision in introns flanking exon80 and thus lead to direct exon80 deletion, we evaluated several sgRNAs in *Col7a1 c.6485G > A mut/mut* keratinocytes in vitro (Fig. S2*B*). Heteroduplex DNA resulting from Cas9/sgRNA-mediated indel formation was detected within most of the tested sgRNAs (Fig. S2*C*). One pair of sgRNAs that exhibited both high cutting efficiency and high specificity was selected for further use (Fig. S2 *D* and *E*). A modified pSpCas9(BB)-2A-EGFP (PX458) plasmid was adopted to express the Cas9 nuclease and both of the sgRNAs (sgRNA-L and sgRNA-R that target, respectively, the 5′ and 3′ introns of exon80) (Fig. S2*F*). Sequencing confirmed the deletion of exon80 at genomic DNA level and mRNA level with high efficiency in vitro (Figs. S2 *G–J*). These results demonstrate that we can use exon deletion to restore the normal function of the collagen VII protein in vivo and demonstrate the suitability of our selected sgRNA pairs to efficiently and specifically delete exon80 of the *Col7a1* locus.

In Vivo Delivered Cas9/sgRNA Ribonucleoproteins via Electroporation Mediates Efficient and Precise DNA Editing in Skin Stem Cells. To have practical and long-term therapeutic effect for our gene correction strategy, it would be essential to adapt the CRISPR/Cas9-mediated gene editing system in postnatal skin stem cells in vivo. We initially tried using electroporation-based delivery of plasmid DNA to the skin of postnatal mice. To unambiguously detect functional DNA delivery in vivo, we used Cre-expressing plasmid in the skin of *Rosa26-stop-tdTomato* reporter mice. Successfully delivering DNA into the skin cells in vivo would lead to Cre-recombinase–mediated excision of the floxed-stop-floxed (lsl) codon and would thus allow tdTomato expression. Cre-expressing plasmids were first intradermally injected into mouse back skin; this step was followed by electroporation. We observed that most of the tdTomato$^+$ cells were present only in the panniculus carnosus of the mouse back skin (Fig. S3 *A–C*). The panniculus carnosus is a sheet of muscle cells underneath the mouse back skin dermis; it is vestigial or absent in human skin (31). To circumvent this problem, we switched to newborn mouse tail skin, which has a thick epidermis and no panniculus carnosus, similar to human skin. Using the same optimized electroporation conditions, whole mount staining clearly revealed tdTomato$^+$ cells in the epidermis (Fig. S3 *D* and *E*). The same in vivo electroporation method also works efficiently to deliver plasmid into adult mouse tail skin (Fig. S3*I*).

Next, we used a plasmid expressing Cas9-2A-EGFP and could easily detect abundant GFP$^+$ cells in whole mount tail skin epidermis at 2 d posttreatment (Fig. S3 *F–H*). However, upon closer inspection, most if not all of the GFP$^+$ cells were located in the stratum corneum; none were present in the basal epidermal layer where stem cells locate (Fig. S3*H*). Similar results were observed using a plasmid expressing the Cas9 nuclease and two sgRNAs targeting the floxed stop codon in *Rosa26-stop-tdTomato* reporter mice, which are termed sgRNA lsl-L and lsl-R, respectively (Fig. 3 *A–C*). So, even though the plasmid delivery method worked in vivo, its failure to target either epidermal stem cells or dermal fibroblasts renders this method ineffective for use in gene therapy applications.

Cas9/sgRNA ribonucleoproteins have been reported to have a higher rate of cleavage and clearance compared with plasmid DNA in in vitro cell culture systems (32). When high-purity recombinant Cas9 and in vitro-transcribed sgRNAs lsl-L and lsl-R were electroporated into *Rosa26-stop-tdTomato* keratinocytes, as high as 70% of cells expressed tdTomato (Fig. S3 *J* and *K*). Previous reports used lipid-mediated delivery of Cas9/sgRNA complexes into the mouse inner ear in vivo, resulting in genome modification in ear hair cells (33). Here we used electroporation to deliver Cas9/sgRNA ribonucleoproteins into intact mouse tail skin. Unlike the results observed in our DNA plasmid electroporation experiments, this combination resulted in efficient targeting of cells in all layers of the epidermis, including in the basal epidermis (Fig. 3 *D–F*). The earliest detectable tdTomato expression occurred 22 h after electroporation (Fig. 3*G*). At 48 h after one electroporation treatment, dramatically higher numbers of basal and suprabasal epidermal cells expressed tdTomato, compared with the very low efficiency using plasmid DNA (Fig. 3 *G* and *H*). Because epidermis is a tissue with fast cellular turnover rate during normal homeostasis, to have long-term therapeutic effect following gene correction in vivo, it is essential that skin stem cells with long-term self-renewing ability are targeted for gene editing so that they can

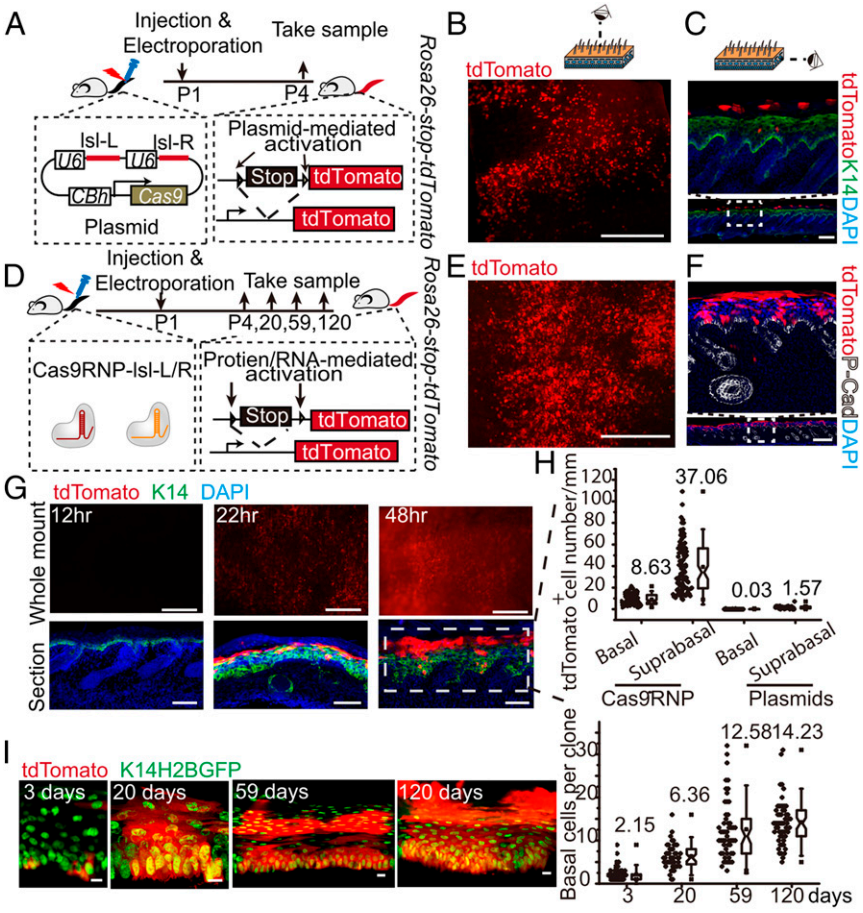

Fig. 3. Efficient in vivo deliveries of Cas9/sgRNA ribonucleoproteins into skin stem cells of postnatal mice using electroporation. (*A*) Schematic diagram of electroporation with pSpCas9-lsl-L/R plasmid at the tail of *Rosa26-stop-tdTomato* reporter newborn mice. Representative whole mount (*B*) and section (*C*) immunofluorescence staining of *Rosa26-stop-tdTomato* mouse tail skin after pSpCas9-lsl-L/R plasmid electroporation. (Scale bar, 1 mm for whole mount images, 100 μm for section staining images.) (*D*) Schematic diagram of electroporation with Cas9/sgRNA ribonucleoproteins at the tails of *Rosa26-stop-tdTomato* reporter newborn mice. Representative whole mount (*E*) and section (*F*) immunofluorescence staining of *Rosa26-stop-tdTomato* reporter tail skin at 3 d after treatment. (Scale bar, 1 mm for whole mount images, 500 μm for section staining images.) (*G*) Representative whole mount and section immunofluorescence stainings of *Rosa26-stop-tdTomato* reporter tail skin at 12 h, 22 h, and 48 h post-Cas9/sgRNA ribonucleoprotein electroporation. (Scale bar, 500 μm for whole mount images, 70 μm for section images.) (*H*) Quantifications of the number of tdTomato$^+$ cells in the basal and suprabasal layers of epidermis at 3 d post-electroporation treatments with either ribonucleoproteins or plasmid DNA. (*I*) Expansion of basal cell per colony after one electroporation treatment with Cas9/sgRNA ribonucleoproteins. Representative images at 3, 20, 59, and 120 d posttreatment are shown at *Left*; quantifications are shown at *Right*. (Scale bar, 10 μm.)

continuously produce functional collagen VII. To determine whether epidermal stem cells were targeted successfully, we followed the long-term fate of the labeled basal epidermis cells after one electroporation and found that up to 120 d later the basal cell colonies laterally expanded and gave continuous progenies in all of the upper epidermis layers (Fig. 3*I*). These results strongly indicate that we are able to efficiently deliver Cas9/sgRNA ribonucleoproteins into postnatal skin stem cells in live animals, which is a prerequisite for carrying out effective gene correction therapies in vivo.

Cas9/sgRNA Ribonucleoproteins Mediated in Vivo Exon80 Deletion in *Col7a1 c.6485G > A mut/mut* Mice Rescues Skin Defects. Combining the exon skipping gene correction strategy and the in vivo Cas9/sgRNA ribonucleoproteins delivery system, we carried out the curative gene editing treatment in our postnatal RDEB mutant mice. Cas9/sgRNA ribonucleoproteins targeting exon80 of the *Col7a1* locus were injected intradermally into *Col7a1 c.6485G > A mut/mut* mouse tail skin at P1 or P2, followed by electroporation. To isolate the target cells for sequence analysis, *Rosa26-stop-tdTomato* allele was bred into the mutant mouse line and Cas9/sgRNA ribonucleoproteins targeting the floxed stop codon of *tdTomato* were injected simultaneously during treatment. Tail skin samples were analyzed 3–5 d posttreatment (Fig. 4*A*). Fluorescence-activated cell sorting (FACS) isolated tdTomato$^+$ cells were used for genomic DNA and mRNA sequence analysis. Truncated genomic DNA resulting from Cas9/sgRNA-mediated excision was detected in gene-corrected skin samples, and sequencing results revealed the successful deletion of *Col7a1* exon80 (Fig. 4*B*). RT-PCR of transcripts from gene-corrected skin samples also revealed deletion of exon80 at the mRNA level (Fig. 4*C*). To estimate the efficiency of in vivo gene editing in our mutant mice, percentage of tdTomato$^+$ cells in whole epidermis after a single treatment was quantified by FACS, and ∼2% epidermal cells were targeted (Fig. 4*D*). We next examined the collagen VII protein distribution patterns in vivo using immunofluorescence staining (Fig. 4 *E* and *F*). In WT skin treated with PBS injection and electroporation, collagen VII proteins localized at the BMZ in a linear pattern. Although *Col7a1 c.6485G > A wt/mut* mice have functionally normal skin, the collagen VII proteins of these mice were distributed at the BMZ in a linear pattern as well as scattered throughout the rest of the skin in a dotted pattern. This phenomenon suggests as long as there are functional collagen VII protein forming anchoring fibrils at the BMZ, the intact adhesion of epidermis to dermis will be maintained, despite the presence of defective collagen VII protein elsewhere in the skin. When Cas9/sgRNA ribonucleoproteins targeting *Col7a1* exon80 were injected intradermally into the *Col7a1 c.6485G > A mut/mut* mouse tail skin followed by electroporation, there was clear enrichment of collagen VII localization at the BMZ 3–5 d later, a phenomenon not observed when *Col7a1 c.6485G > A mut/mut* mice skin was treated with the control PBS injection and electroporation. We quantified these changes in the distribution of collagen VII using Nidogen as a marker for where the BMZ is (Fig. 4*F*). The ratio of fluorescence intensities of collagen VII at the BMZ and neighboring lower dermis showed significant increase after one treatment with Cas9/sgRNA ribonucleoproteins in the *Col7a1 c.6485G > A mut/mut* mice skin. Under the same measurement condition, the ratio of fluorescence intensity for Nidogen did not show difference, thus excluding the possibility of measurement bias. As the ultimate functional test for the in vivo gene editing efficiency in our RDEB mice, we measured the degree of

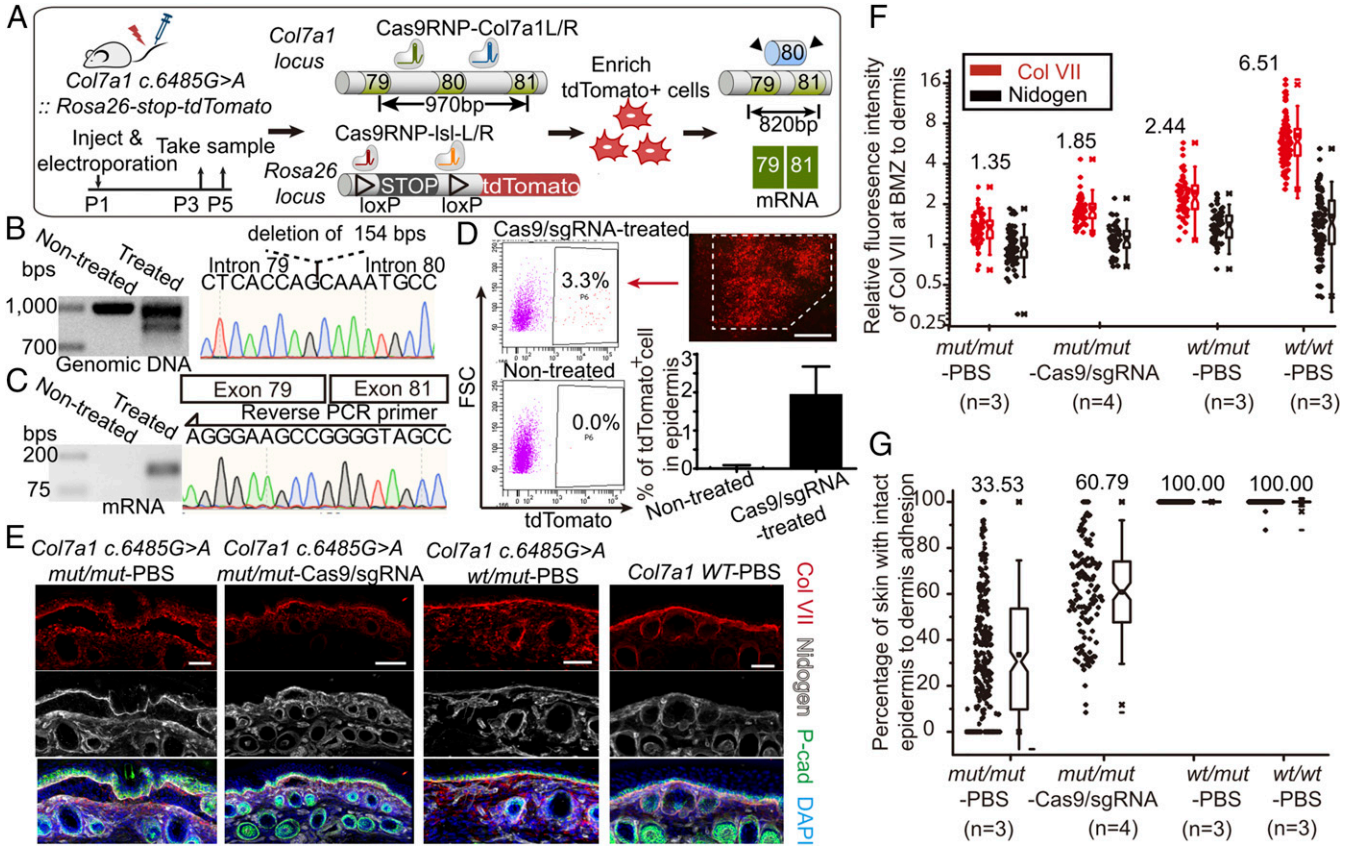

Fig. 4. Cas9/sgRNA ribonucleoprotein-mediated in vivo gene editing in postnatal RDEB mice. (*A*) Schematic diagram *of* in vivo gene editing in *Col7a1 c.6485G > A::Rosa26-stop-tdTomato* mice. (*B*) PCR amplifications of the *Col7a1* genomic DNA from FACS isolated in vivo tdTomato$^+$ cells demonstrate truncation at exon80 after treatment. Partial *Col7a1* gene sequencing result shows the deletion of exon80. (*C*) RT-PCR of *Col7a1* mRNA from FACS isolated in vivo tdTomato$^+$ cells indicates deletion of exon80, confirmed by sequencing result of the *Col7a1* mRNA. (*D*) FACS analysis of the percentage of tdTomato$^+$ cells in epidermis of *Col7a1 c.6485G > A::Rosa26-stop-tdTomato* mice at day 2 posttreatment. (Scale bar, 1 mm.) (*E*) Immunofluorescence stainings of Col VII, P-cad, and Nidogen in *Col7a1 c.6485G > A mut/mut, wt/mut* and WT tail skins with indicated electroporation treatments with either PBS or Cas9/sgRNA ribonucleoproteins targeting *Col7a1* exon80. (Scale bar, 50 μm.) (*F*) Relative fluorescence intensity of Col VII at BMZ compared with lower dermis. Nidogen marks the location of BMZ and its quantification serves as a quantification control. (*G*) Percentage of skin with intact epidermis-to-dermis adhesion in different samples.

the epidermis-to-dermis adhesion. Both WT and the *Col7a1 c.6485G > A wt/mut* skin had 100% adhesion between the epidermis and the dermis. After one treatment with Cas9/sgRNA ribonucleoproteins, the average adhesion area of *Col7a1 c.6485G > A mut/mut* skin increased from ∼30% to ∼60% (Fig. 4*G*). All these findings provide direct evidence that Cas9/sgRNA ribonucleoproteins can efficiently mediate gene editing for RDEB at the genomic DNA, mRNA, protein, and phenotypic levels.

It is worth noting that the effects described above were observed only 3–5 d following a single treatment. Whether or not the corrective effect lasts over the long term is a key remaining question. And given the fact that we observed the long-term expansion of basal cell colonies following treatment, it will be interesting to see whether the correction efficiency may actually increase over time. To circumvent the problem of early postnatal lethality of the *Col7a1 c.6485G > A mut/mut* mice, we tried grafting the tail skin onto nude mice to pursue long-term analysis. Both WT and mutant skin grafts survived on the backs of nude mice. However, it became obvious that the epidermis-to-dermis adhesion defect in mutant skin was rescued on the backs of nude mice over time without treatment (Fig. S4 *A*–*C*). Immunofluorescence staining revealed the presence of mouse collagen VII protein at the BMZ close to the edge of the graft, and this pattern expanded even further into the center of the graft at later time points (Fig. S4 *A* and *C*). This phenomenon made the long-term characterization of the gene correction effect impossible in these grafted tissues. However, it offers additional evidence supporting that not all of the mutant cells need to be genetically corrected to functionally rescue RDEB, because the secreted functional collagen VII protein from gene-corrected cells can spread to neighboring tissues to rescue the skin blistering defect.

Discussion

Although several gene and cell therapies have been developed to deliver functional collagen VII protein to the RDEB tissue, no curative treatment exists for this disease as yet. In this study, we developed a therapeutic strategy based on the Cas9/sgRNA ribonucleoprotein-mediated gene editing system to restore collagen VII protein function in postnatal RDEB mice. The strategy creates an in-frame deletion of the genomic DNA covering exon80 that commonly harbors the recessive point mutation known to be responsible for the disease. Our results demonstrate that Cas9/sgRNA ribonucleoproteins mediate gene editing efficiently excising targeted genomic DNA in skin stem cells in postnatal animals. This restores the function of the collagen VII protein, correcting the epidermis–dermis adhesion defect.

The Cas9/sgRNA ribonucleoprotein-based gene therapy developed here has several advantages over traditional gene/cell therapies and virus-based CRISPR gene-editing systems. First, our Cas9/sgRNA ribonucleoprotein-based gene therapy works at

the genomic level in stem cells in vivo. This implies long-term effectiveness in restoring the defective gene and should obviate the need for repeated treatment over time. Also, because this therapy works in intact somatic tissue in vivo, the complexity and full function of the tissue is maintained. These advantages would significantly reduce the cost and complications associated with traditional gene or cell therapies for RDEB. Second, using the nonreplicable protein/RNA complexes as gene editing system in vivo circumvents multiple drawbacks associated with virus-based delivery systems described earlier.

At the same time, several issues still remain for this in vivo gene editing system. First of all, our current electroporation system can only be applied to local skin areas, and the percentage of targeted cells after a single treatment still needs to be improved. Even though we do see significant effect in terms of restoration of correct collagen VII protein localization and improvement of skin adhesion in the treated area, further optimization of the delivery condition that can increase the target area as well as editing efficiency will have profound clinical impact. Secondly, whether or not this gene editing system can result in effective treatment over the long term needs to be addressed. Other skin disease mouse models that do not result in early postnatal lethality or do not involve secreted protein can circumvent our current technical problem. Additionally the human RDEB skin model generated ex vivo and grafted onto nude mice can be used to address the long-term effect question, and it will also provide a necessary system to study whether the condition developed here can also be applied to human skin tissue. Last but not least, even though the electroporation is performed immediately after ribonucleoprotein complex injection, the potential in vivo immunogenicity against the injected ribonucleoprotein complexes needs to be addressed when multiple injections might be needed to achieve sufficient genome editing in vivo.

In sum, our study provides proof-of-principle evidence that Cas9/sgRNA ribonucleoprotein-based gene therapies can be applied to restore collagen VII protein function in postnatal RDEB mice, suggesting that the Cas9/sgRNA ribonucleoprotein-based gene editing system may offer curative treatment for RDEB and other genetic disorders.

Materials and Methods

Detailed materials and methods are provided in *SI Materials and Methods*.

All mice were maintained in an specific pathogen-free (SPF) facility, and procedures were conducted in a manner consistent with the National Institute of Biological Sciences Guide for the Care and Use of Laboratory Animals. For the offspring identification, genotyping was performed using specific primers against mutant allele and WT allele, respectively. The 1.5-kb donor harboring the c.6485G > A mutation as well as a "CGACC" insertion within an intron was generated by PCR. The pSpCas9(BB)-2A-GFP (PX458, plasmid 48138) plasmid was purchased from Addgene. The CMV promoter-driven pLJM1-Cre plasmid was modified from the pLJM1-EGFP (Addgene, plasmid 19319) plasmid. The sgRNAs were designed using the on-line CRISPR design tool of Feng Zhang's laboratory (crispr.mit.edu/). Primary keratinocytes were isolated from newborn back skin. Lipofectamine 2000 (Thermo Fisher Scientific) was used to transfect keratinocyte cells with plasmids. Within in vitro keratinocytes, Cas9/sgRNA complexes were electroporated with neon electroporation system (Thermo Fisher Scientific). T7 endonuclease I assay was used to detect sgRNA function in vitro. In vitro transfected keratinocytes and in vivo treated skin were analyzed and enriched by fluorescence-activated cell sorting with standard procedures. Genomic DNA was extracted with a TIAMamp genomic DNA kit (TIANGEN). Total RNA was isolated using a direct-Zol RNA mini prep kit (Zymo Research) and reverse transcripted into cDNA with reverse-transcriptase reaction mix (Takara). Single colony sequencing was performed to detect indels within genome and mRNA. Recombinant Cas9 was expressed using pET28-b(+)-Cas9 transformed into BL21(DE3). The Cas9 protein was purified using Ni-NTA agarose resin (Qiagen). SgRNA was transcripted using a MEGAscript T7 Transcription kit (Thermo Fisher Scientific) and purified with a Gel DNA Recovery kit (Zymo Research). In vivo mice electroporation experiments were performed with a square wave pulse generator (ECM 830). Standard cryosection fluorescence staining and hematoxylin and eosin (H&E) staining procedures were performed to detect protein expression in indicated tissue. Digital images were acquired by confocal microscope and processed by Imaris software. Each newborn *Col7a1 c.6485G > a mut/mut* mouse tail skin together with a WT littermate tail skin was grafted onto the same CD1 nude mouse back skin. Box-and-whisker plots were prepared with Origin 9 software (OriginLab), which was also used in the statistical analysis of data. GraphPad Prism 6 software was used to make the survival curves and histograms.

1. Cong L, et al. (2013) Multiplex genome engineering using CRISPR/Cas systems. *Science* 339(6121):819–823.
2. Doudna JA, Charpentier E (2014) Genome editing. The new frontier of genome engineering with CRISPR-Cas9. *Science* 346(6213):1258096.
3. Mali P, et al. (2013) RNA-guided human genome engineering via Cas9. *Science* 339(6121):823–826.
4. Maddalo D, et al. (2014) In vivo engineering of oncogenic chromosomal rearrangements with the CRISPR/Cas9 system. *Nature* 516(7531):423–427.
5. Yin H, et al. (2014) Genome editing with Cas9 in adult mice corrects a disease mutation and phenotype. *Nat Biotechnol* 32(6):551–553.
6. Swiech L, et al. (2015) In vivo interrogation of gene function in the mammalian brain using CRISPR-Cas9. *Nat Biotechnol* 33(1):102–106.
7. Chiou SH, et al. (2015) Pancreatic cancer modeling using retrograde viral vector delivery and in vivo CRISPR/Cas9-mediated somatic genome editing. *Genes Dev* 29(14): 1576–1585.
8. Tabebordbar M, et al. (2016) In vivo gene editing in dystrophic mouse muscle and muscle stem cells. *Science* 351(6271):407–411.
9. Long C, et al. (2016) Postnatal genome editing partially restores dystrophin expression in a mouse model of muscular dystrophy. *Science* 351(6271):400–403.
10. Nelson CE, et al. (2016) In vivo genome editing improves muscle function in a mouse model of Duchenne muscular dystrophy. *Science* 351(6271):403–407.
11. Lunstrum GP, Sakai LY, Keene DR, Morris NP, Burgeson RE (1986) Large complex globular domains of type VII procollagen contribute to the structure of anchoring fibrils. *J Biol Chem* 261(19):9042–9048.
12. Sakai LY, Keene DR, Morris NP, Burgeson RE (1986) Type VII collagen is a major structural component of anchoring fibrils. *J Cell Biol* 103(4):1577–1586.
13. Uitto J, Pulkkinen L (1996) Molecular complexity of the cutaneous basement membrane zone. *Mol Biol Rep* 23(1):35–46.
14. Burgeson RE (1993) Type VII collagen, anchoring fibrils, and epidermolysis bullosa. *J Invest Dermatol* 101(3):252–255.
15. Bruckner-Tuderman L (2010) Dystrophic epidermolysis bullosa: Pathogenesis and clinical features. *Dermatol Clin* 28(1):107–114.
16. Remington J, et al. (2009) Injection of recombinant human type VII collagen corrects the disease phenotype in a murine model of dystrophic epidermolysis bullosa. *Mol Ther* 17(1):26–33.
17. Woodley DT, et al. (2004) Injection of recombinant human type VII collagen restores collagen function in dystrophic epidermolysis bullosa. *Nat Med* 10(7):693–695.
18. Ortiz-Urda S, et al. (2003) Injection of genetically engineered fibroblasts corrects regenerated human epidermolysis bullosa skin tissue. *J Clin Invest* 111(2):251–255.
19. Woodley DT, et al. (2003) Normal and gene-corrected dystrophic epidermolysis bullosa fibroblasts alone can produce type VII collagen at the basement membrane zone. *J Invest Dermatol* 121(5):1021–1028.
20. Wong T, et al. (2008) Potential of fibroblast cell therapy for recessive dystrophic epidermolysis bullosa. *J Invest Dermatol* 128(9):2179–2189.
21. Gache Y, et al. (2004) Construction of skin equivalents for gene therapy of recessive dystrophic epidermolysis bullosa. *Hum Gene Ther* 15(10):921–933.
22. Chen M, et al. (2002) Restoration of type VII collagen expression and function in dystrophic epidermolysis bullosa. *Nat Genet* 32(4):670–675.
23. Ortiz-Urda S, et al. (2002) Stable nonviral genetic correction of inherited human skin disease. *Nat Med* 8(10):1166–1170.
24. Sebastiano V, et al. (2014) Human COL7A1-corrected induced pluripotent stem cells for the treatment of recessive dystrophic epidermolysis bullosa. *Sci Transl Med* 6(264):264ra163.
25. Wenzel D, et al. (2014) Genetically corrected iPSCs as cell therapy for recessive dystrophic epidermolysis bullosa. *Sci Transl Med* 6(264):264ra165.
26. Umegaki-Arao N, et al. (2014) Induced pluripotent stem cells from human revertant keratinocytes for the treatment of epidermolysis bullosa. *Sci Transl Med* 6(264): 264ra164.
27. Bilousova G, Roop DR (2014) Induced pluripotent stem cells in dermatology: Potentials, advances, and limitations. *Cold Spring Harb Perspect Med* 4(11):a015164.
28. Ferrari S, Pellegrini G, Matsui T, Mavilio F, De Luca M (2006) Towards a gene therapy clinical trial for epidermolysis bullosa. *Rev Recent Clin Trials* 1(2):155–162.
29. Kiuru M, Itoh M, Cairo MS, Christiano AM (2010) Bone marrow stem cell therapy for recessive dystrophic epidermolysis bullosa. *Dermatol Clin* 28(2):371–382, xii–xiii.
30. Wagner JE, et al. (2010) Bone marrow transplantation for recessive dystrophic epidermolysis bullosa. *N Engl J Med* 363(7):629–639.
31. Naldaiz-Gastesi N, et al. (2016) Identification and characterization of the dermal panniculus carnosus muscle stem cells. *Stem Cell Reports* 7(3):411–424.
32. Liang X, et al. (2015) Rapid and highly efficient mammalian cell engineering via Cas9 protein transfection. *J Biotechnol* 208:44–53.
33. Zuris JA, et al. (2015) Cationic lipid-mediated delivery of proteins enables efficient protein-based genome editing in vitro and in vivo. *Nat Biotechnol* 33(1):73–80.